Evaluation of the inverse dynamic model in cerebellum during visual-vestibular interactions at different VOR gains in squirrel monkeys

Yutaka Hirata[1], Akimasa Yoshikawa[1], Pablo M. Blazquez[2], Stephen M. Highstein[2]

[1] Dept. Electronic Engineering, Chubu University College of Engineering,
[2] Dept. Otolaryngology, Washington University School of Medicine

Abstract Generality of the cerebellar inverse dynamic model (IDM) theory was evaluated in oculomotor control in squirrel monkeys. Flocculus Purkinje cell firing patterns recorded during visual, vestibular and their interaction paradigms at various VOR gains were reconstructed by the IDM consisting of the linear combination of eye position, velocity, and acceleration. The IDM could successfully reconstruct more than 72 % of the firing patterns of 138 cells, but with different sets of parameters for different paradigms and different VOR gains. This result suggests that the output of the flocculus relates to motor output, but not the motor command per se.

Keywords: Cerebellum, Purkinje cell, Inverse dynamic model, VOR, Motor leaning, Monkey

1. Introduction

It is widely accepted that one of the main roles of the cerebellum is the organization of movement, but how the cerebellum achieves this function has been a matter of debate. A successful theory is the inverse dynamic model hypothesis that states that the cerebellum adaptively forms the inverse dynamic model of the muscle plant that is innervated by corresponding cerebellar region via deep cerebellar nuclei or vestibular nuclei [7]. The inverse dynamic model receives a desired trajectory as an input and outputs the motor command or its equivalent that drives the muscle plant and produces the desired trajectory. In support of this theory, Shidara et al. [11] and Gomi et al. [3] have shown in a monkey eye movement control called ocular following response (OFR) that the firing patterns of ventral parafloccu-lus Purkinje cell simple spike encode information equivalent to the dynamic components (velocity and acceleration) of the motor command carried by oculomotor motoneurons. The OFR is a visually-driven eye movement that is elicited by the velocity step of a random dots pattern. The results from other laboratories support this hypothesis in other visually-driven eye movement controls in cat optokinetic response (OKR) [9], monkey OKR [4] and monkey smooth pursuit [12]. Currently we test the generality of the inverse dynamic model theory in oculomotor control in squirrel monkeys by extending the stimulus class to those including vestibular and visual-vestibular interaction paradigms. We also evaluate this theory at the different gains of vestibuloocular reflex (VOR) to test the adaptability of the inverse dynamic model in cerebellum.

2. Methods

Subjects and general experimental procedures

Two adult male squirrel monkeys (M1598, MB46) were utilized in these experiments. They were prepared for chronic flocculus single unit recording, and eye movement measurement using scleral search coils. Details of these methods and the set-up to modify the animals' vertical (V) VOR were same as in the previous reports [2, 5, 6]. Briefly, the animals were trained for at most 7 hours, usually 4 hours, to decrease or increase their VVOR gains defined as slow phase eye velocity/head velocity by using suppression of VOR (VORs) or enhancement of VOR (VORe) paradigm (Figure 1). In some trials, reversal of VOR was used to decrease the gain. In all the paradigms, the chair rotation was a 0.5 Hz

sinusoid with the amplitude of 40 deg/s. Floccular complex (including genuine flocculus and ventral paraflocculus) Purkinje cells were isolated during the training at various VVOR gains. Purkinje cells were identified by the pause of simple spike (SS) after the occurrence of complex spikes (CS) when both SS and CS were recorded simultaneously. When only SS were captured, the unit is considered as a Purkinje cell if we could hear CS through the sound monitor and the estimated parameters of the unit are close to those of other identified Purkinje cells (These putative Purkinje cells are less than 15% of entire population analyzed). When a single unit was isolated, its response to VOR in darkness (VORd), OKR, VORs, and VORe paradigms were applied in addition to no-stimulus in dark and light paradigms (nostimD and nostimL) for 1 min each. After recording all these paradigms, training was continued and the same recording session was repeated every hour until the cell was lost. When a cell was lost, another cell was searched while the training was continued. Experimental protocols were approved by the Washington University Committee on Animal Care and performed in accordance with NIH guidelines.

Data handling

Chair velocity, optokinetic stimulus velocity, horizontal and vertical eye positions were A/D-converted at the sampling rate of 200 Hz each into a PC through the Power 1401 (Cambridge Electronic Design) controlled by Spike2 software. Neuronal data were acquired in two ways; as raw waveform data A/D-converted at the sampling rate of 40 KHz, and as events or spike occurrence times detected in real time using a window discriminator. The data were exported off-line to Matlab (Mathworks) and all the subsequent data handling and analyses were performed on Matlab. Eye velocity and acceleration were calculated by using a low pass differentiation filter from the eye position traces. VOR gain, G_{VOR} was measured as shown by the following equation:

$$v_{eye}(t) = G_{VOR} v_{head}(t - \Delta) + dc + \xi(t)$$

where $v_{eye}(t)$ and $v_{head}(t)$ are the vertical eye and head velocity during VORd, respectively, dc denotes the dc term that was close to 0 in most cases, and $\xi(t)$ is the error term. Δ [s] is the delay time between eye and head velocity. The coefficients G_{VOR} and dc were determined by solving the normal equation derived from the above equation to minimize the square sum of $\xi(t)$ with a given Δ. The value of Δ that gives the minimum square sum of $\xi(t)$ was globally searched. From the event data, firing rate [spikes/sec] was calculated in each time interval whose bin size is 0.005 sec corresponding to the same sampling rate of 200 Hz as other digitized signals. Average eye position, velocity, acceleration and Purkinje cell SS firing rate over 30 cycles (1 min) of the head or optokinetic stimulus rotation were calculated after eliminating saccades with a semi-automated method developed in our laboratory.

The inverse dynamic model

The desaccaded and averaged firing rate $f(t)$ was reconstructed by the same inverse dynamic model as in the previous studies [3, 4, 7, 9, 11, 12]:

$$f(t - \tau) = \alpha \frac{d^2 x(t)}{dt^2} + \beta \frac{dx(t)}{dt} + \gamma x(t) + \delta + \varepsilon(t) \tag{1}$$

where α, β, γ are the coefficients of the desaccaded and averaged eye acceleration, velocity, position $x(t)$, respectively, δ and $\varepsilon(t)$ are dc firing rate and an error term, respectively. τ is

the latency between Purkinje cell firing and eye movement. If τ is positive eye movements lag the Purkinje cell firing. These coefficients were estimated so that the following object function that is a weighted squared sum of residual is minimized:

$$\boldsymbol{o} = \sum_t \boldsymbol{w}(t)\varepsilon^2(t)$$

(2)

where $w(t)$ is the weight function that is a square root of the number of cycles used to calculate the desaccaded and averaged eye and firing rate traces. In this way, we could evaluate the error $\varepsilon(t)$ at each time t by taking account of the reliability of estimated values of the desaccaded and averaged traces. $\alpha, \beta, \gamma, \delta$ were determined by solving the least-squares normal equation derived from Eq.(1) to minimize Eq.(2), while τ was globally searched between –0.05 and 0.05 sec in a 0.001 sec step. Validity of the model was evaluated by a residual check and variance inflation factor (VIF). If VIF is larger than 10, the model was judged invalid due to serious multicollinearity among the regressors. The residual check compares statistical properties (amplitude distribution and autocorrelation function) of the residual $\varepsilon(t)$ with spontaneous Purkinje cell firing pattern measured during no stimulus conditions (nostimD and nostimL) [5]. The idea is that if the statistical properties of $\varepsilon(t)$ are identical to those of the Purkinje cell's spontaneous firing then we can assume that all the signal components induced by vestibular and/or optokinetic stimulus in Purkinje cell firing pattern are extracted by the model. The Lepage test was used to compare the amplitude distributions. The autocorrelation function of residual was judged different from that of spontaneous firing when their difference at any of time shifts exceeded 0.1.

3. Results

Figure 1 illustrates the firing patterns of a typical floccular complex Purkinje cell and the eye movements during VORd, VORe, VORs, and OKR paradigms. This cell was recorded when the animal's VOR gain was normal. Typical Purkinje cells increase their firing rate during downward eye movements and downward head movements, thus modulate out-of-phase with optokinetic stimulus during OKR, out-of-phase with head velocity during VORs, and show little modulation during VORd in which head and eye move in an out-of-phase manner with nearly the same amplitude.
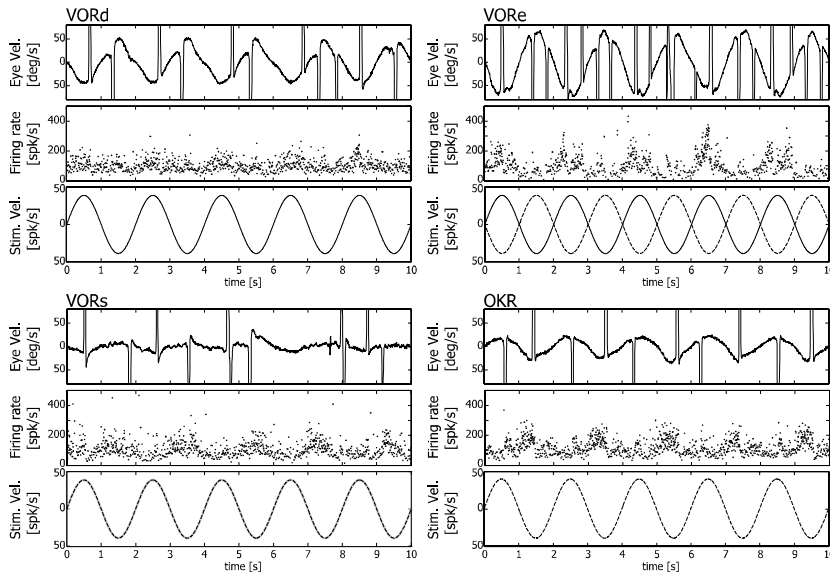

Figure 1: Cerebellar flocculus Purkinje cell firing patterns and vertical eye velocity during the experimental paradigms currently used. In the bottom panels, solid lines indicate head velocity traces while dotted lines indicate optokinetic stimulus (OKS) velocity. During VORd, the animal's head was rotated in dark. During VORe and VORs, OKS was applied out-of-phase and in-phase with the head velocity, respectively. Only OKS was applied during OKR. Positive values in eye and stimulus traces indicate upward motion.

Figure 2 illustrates the examples of the reconstruction of Purkinje cell firing pattern by the inverse dynamic model during each paradigm (columns 1 through 4). In the 1st row, gray traces are the Purkinje cell firing rates desaccaded and averaged over cycles, and black lines are the model reconstruction. The 2nd, 3rd, and 4th rows illustrate vertical eye acceleration, velocity, and position traces, respectively. Thin lines are those of each stimulus cycle while black lines are their averages. The estimated parameters are superimposed in each panel. The 5th row from the top illustrates the weight functions that is the number of cycles at each data point used to calculate the averages. The bottom row shows stimulus waveforms. Out of 368 samples (VORd: 127, VORs: 65, VORe: 80, OKR: 96) from 138 cells (41 cells from M1598, 97 cells from MB46), all the samples yielded VIF less than 10, and 72 % (VORd: 71 %, VORs: 62 %, VORe: 76 %, OKR: 77 %) passed the residual check. Further analyses were done on those that passed the residual check.
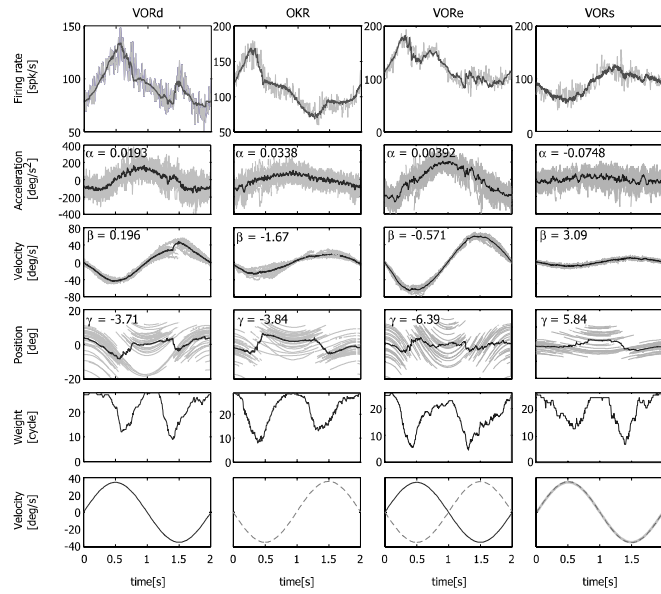
Figure 2: Reconstruction of Purkinje cell firing pattern during each paradigm by the inverse dynamic model. Note in the top panels that the model reconstruction (black line) fits to the Purkinje cell firing pattern in each paradigm. The numbers in the 2nd, 3rd, and 4th rows are the parameter values of eye acceleration, velocity and position term of the model, respectively estimated to optimally reconstruct the firing pattern during each paradigm.
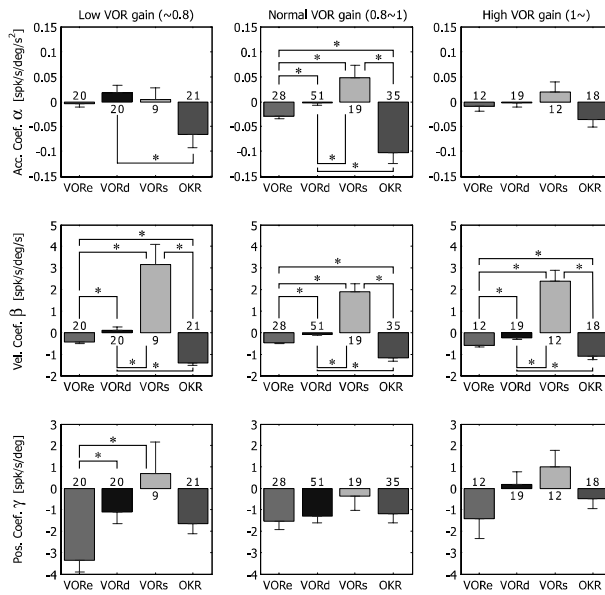
Figure 3: The averages of parameter values during each paradigm in different VOR gain groups (low, normal, and high VOR gains). Error bars indicate one standard deviation. The number of samples in each condition is indicated below or above each bar. Asterisks indicate statistically significant difference (Steel-Dwass' test *: $p < 0.05$).

Figure 3 summarizes the estimated parameters of the inverse dynamic model. The parameters estimated from each paradigm are compared in each VOR gain group, namely low (~0.8), normal (0.8~1.0), and high gain (1.0~). Error bars indicate one standard deviation.

Asterisks indicate statistically significant difference in each VOR gain group (Steel-Dwass' multiple comparison, *: p<0.05). The statistical test revealed that any combinations of the averages of eye velocity coefficient β from 4 different paradigms are different in each VOR gain group. The same is true for eye acceleration parameter α in the normal VOR gain group. In contrast, eye position parameter γ does not show such paradigm dependency except for VORe in the low VOR gain group. In the low and high VOR gain groups, eye acceleration parameter α does not show paradigm dependency either, except between VORd and OKR in the low gain group. Thus, different sets of parameters, especially for eye velocity coefficient β are required to reconstruct the neuronal firing patterns during different paradigms in each VOR gain group. Further, it is noted in all VOR gain groups that the average velocity coefficients β from VORe has the opposite sign to that from VORs while that from VORd is close to 0. The dependency of the estimated parameters on VOR gain was also found (data not shown). The linear regression of the parameter values against VOR gain revealed statistically significant slope in the velocity coefficient β from VORd, VORe and OKR, and in the eye position coefficient γ from VORd and VORe. No VOR gain dependency was found in the eye acceleration coefficient α from all the paradigms.

4. Conclusions

The cerebellar inverse dynamic model theory predicts that the output of the cerebellum, i.e., Purkinje cell firing, is equivalent to the motor command. The theory was proved plausible for visually-driven eye movement control [3, 11], and useful for actual robot arm control [1]. Currently we tested generality of this theory in eye movement control by extending the stimulus class to those including vestibular and visual-vestibular interaction stimuli. If cerebellar output were to meet the conditions specified by the inverse dynamic model theory the parameter set should be constant for all behavioral conditions. The visual-vestibular interaction stimuli currently employed (VORs, VORe) induce VOR motor learning in which the inverse dynamic model should recalibrate its characteristics to generate appropriate eye movements. During VORs, eyes tend to move faster than required, thus the motor command should be smaller than that during the normal situation, i.e. VORd or OKR. The opposite should be the case during VORe, in which larger motor command is required. The current results only partially support this prediction in that Purkinje cell modulation during VORe is in the opposite direction to that during VORs, and during VORd the cell modulation is close to 0. Stimuli consisting of visual or vestibular component alone, that is, OKR and VORd, do not induce VOR motor learning in primates. Thus the current result that different parameter sets are required for these two paradigms again does not support the idea that the output of the flocculus is motor command by itself. Then, what does the floccular output encode? The fact that most of the flocculus Purkinje cell firing patterns could be reconstructed by the inverse dynamic model albeit with different sets of parameters suggests that the output of the flocculus is related to the motor command. It has been proposed that floccular output is employed as an error signal for its target neurons (FTNs) in vestibular nucleus and dorsal Y group [8] where causal changes in neuronal firing patterns have been found along with VOR motor learning [10]. Our results suggest that this error signal is in the same coordinate frame as the motor command that represents the elastic, viscous, and inertial components of the oculomotor muscle plant. The eye acceleration, velocity and position components in floccular output may inform the FTNs how much the deficit/excess is in each component of motor command, and let them learn to generate the appropriate motor command that is directly sent to the oculomotor motoneurons where the final motor command is generated.

Acknowledgements

References

[1] G. Atkeson, J. G. Hale, F. Pollick, M. Riley, S. Kotosaka, S. Schaal, T. Shibata, G. Tevatia, A. Ude, S. Vijayakumar, M. Kawato, Using humanoid robots to study human behavior, IEEE Intelligent Systems: Special Issue on Humanoid Robotics. 15(2000) 46-56.

[2] P. M. Blazquez, Y. Hirata, S. A. Heiney, A. M. Green, S. M. Highstein, Cerebellar signatures of vestibulo-ocular reflex motor learning, J. Neurosci. 23(2003) 9742-9751.

[3] H. Gomi, M. Shidara, A. Takemura, Y. Inoue, K. Kawano, M. Kawato, Temporal Firing Patterns of Purkinje Cells in the Cerebellar Ventral Paraflocculus during Ocular Following Responses in Monkeys I. Simple Spikes, J. Neurophysiol. 80(1998) 818-831.

[4] Y. Hirata, R. Arikan, and S.M. Highstein, Multiple linear regression analysis of floccular purkinje cell activity during vertical visual following in squirrel monkeys, 28th Soc. Neurosci Abst. 24, p.1405

[5] Y. Hirata and S.M. Highstein, Acute adaptation of the vestibuloocular reflex: signal processing by foccular and ventral parafloccular Purkinje cells, J. Neurophysiol. 85(2001) 2267-2288.

[6] Y. Hirata, J. M. Lockard, S. M. Highstein, Capacity of vertical VOR adaptation in squirrel monkey. J. Neurophysiol. 88(2002) 3194-3207.

[7] M. Kawato and H. Gomi, A computational model of four regions of the cerebellum based on feedback-error learning, Biol Cybern. 68(1992) 95-103.

[8] F. A. Miles, S. G. Lisberger, Plasticity in the vestibulo-ocular reflex: a new hypothesis. Annu Rev Neurosci 4(1981): 273-299.

[9] T. Omata, T. Kitama, A. Mizukoshi, T. Ueno, M. Kawato, Y. Sato, Purkinje cell activity in the middle zone of the cerebellar flocculus during optokinetic and vestibular eye movement in cats. Jpn J Physiol. 50(2000) 357-370.

[10] A. M. Partsalis, Y. Zhang, S. M. Highstein, Dorsal Y group in the squirrel monkey. II. Contribution of the cerebellar flocculus to neuronal responses in normal and adapted animals. J. Neurophysiol. 73(1995) 632-650.

[11] M. Shidara, K. Kawano, H. Gomi and M. Kawato, Inverse dynamics model eye movement control by Purkinje cells in the cerebellum, Nature 365(1993) 50-52.

[12] M. Suh, H.-C. Leung, and R. E. Kettner, Cerebellar flocculus and ventral paraflocculus Purkinje cell activity during predictive and visually driven pursuit in monkey. J Neurophysiol. 84(2000) 1835-1850.

Yutaka Hirata received his B.S. from the Dept of Electrical and Electronic Engineering of Toyohashi Univ. of Technology in 1990, completed the M.E. in 1992 and the Doctor of Engineering in system information engineering in 1995. He then became an invited scientist of Japanese space agency (NASDA). In 1997 he became a postdoctoral fellow at Washington Univ. School of Medicine. In 2000, he joined Chubu Univ. College of Engineering and is currently a full professor of Dept. Computer Science.

Akimasa Yoshikawa received his B.S. degree from the Department of Electronic Engineering of Chubu University College of Engineering in 2002. Currently he is a graduate student of the Dept of Electrical Engineering of Chubu University.

Pablo M. Blazquez studied biology at Seville University and graduated in 1992. From 1991 to 1995 he studied learning in the classical condition reflex at Seville University. From 1994 to 1997 he studied VOR physiology at Washington University in St. Louis. In 1998 he obtained his Ph.D. from Seville University. In 1998 he went to MIT as a postdoctoral fellow and studied mechanisms of motor learning in the striatum. In 2001 he returned to Washington University where he currently holds a research assistant professor position.

Stephen M. Highstein received his B.S in biology from Rensselaer Polytechnic Inst., M.D. from Univ. of Maryland Med. School, and Ph.D. from Univ. of Tokyo Fac. Med. He was an assistant professor from 1974 to 76, associate professor from 76 to 81 and professor from 81 to 83 in Neuroscience at Albert Einstein College of Medicine. He has been a professor of Otolaryngology, Anatomy & Neurobiology, Washington University School of Medicine, St. Louis.